JACS Au
AN OPEN ACCESS JOURNAL OF THE AMERICAN CHEMICAL SOCIETY

pubs.acs.org/jacsau
Perspective

Molecular Design of Al(II) Intermediates for Small Molecule Activation

Published as part of JACS Au special issue "Advances in Small Molecule Activation Towards Sustainable Chemical Transformations".

Roushan Prakash Singh and Neal P. Mankad*

Cite This: *JACS Au* 2025, 5, 2076–2088
Read Online
ACCESS | Metrics & More | Article Recommendations

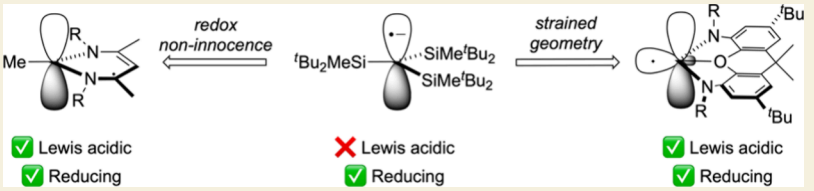

ABSTRACT: Promoting societally important small molecule activation processes with earth-abundant metals is foundational for a sustainable chemistry future. In this context, mapping new reaction pathways that would enable abundant main-group elements to mimic the behaviors of *d*- and *f*-block elements is facilitated by exploring unusual oxidation states. The most abundant metal on earth, aluminum, has been well studied in the Lewis acidic +III and Lewis basic +I oxidation states but rarely in the potentially biphilic +II oxidation state until recently, when a renaissance of Al(II) chemistry emerged from a range of research groups. In this Perspective, we review the chemistry of mononuclear Al radicals, including both Al-centered radicals (i.e., Al(II) compounds) and redox non-innocent systems (i.e., formally Al(II) species that are physically Al(III) with ligand-centered radicals), with an emphasis on small molecule reactivity. We also provide a meta-analysis of the Al(II) literature to summarize how different design strategies (e.g., redox non-innocence, strained coordination geometries) have been shown to impart biphilic character to Al radicals and tune their behavior, thus allowing Al radicals to mimic the chemistry of certain *d*- and *f*-block metal ions such as Ti(III) and Sm(II). We expect these molecular design concepts to inform future Al(II) studies as the chemistry of this unusual oxidation state of Al continues to grow.

KEYWORDS: *Aluminum, radicals, small molecule activation, carbon dioxide, low-valent, main group*

INTRODUCTION

Addressing societal problems like renewable energy storage/conversion and climate change mitigation depends on chemical activation of gaseous small molecules that are inert and/or thermodynamically stable.[1] Fundamentally, use of *d*- and *f*-block metals for small molecule activation tends to be the most efficient approach, especially in catalytic scenarios, due to availability of multiple oxidation states, ligand field tunability, and/or the ability to promote multielectron redox transformations. However, in many cases, this approach also faces sustainability challenges due to the low earth abundance and high commercial cost associated with many of these metals. Therefore, it is imperative to identify ways to promote efficient small molecule activation reactions with the most abundant elements on earth.[2]

The most abundant metal is the *p*-block element, aluminum (Al). The reaction chemistry of Al plays crucial roles in both organic and organometallic synthesis.[3−7] Due to the [Ne]-$3s^2 3p^1$ electronic configuration of elemental Al, molecular compounds typically feature aluminum in the +III oxidation state that achieves a noble gas configuration. The reaction chemistry of Al(III) compounds primarily involves three-coordinate species functioning as Lewis acids and also includes important roles in polymerization catalysis and transmetalation reactions.[8−10] Over the last ∼25 years, it has been established that molecular compounds of Al(I) can also be studied with suitable supporting ligands.[11−15] In contrast to Al(III), Al(I) compounds tend to act as Lewis bases. Compared to the Al(III) and Al(I) oxidation states, Al(II) is rarely studied and may hold the potential for discovering new reaction pathways. Formally Al(II) complexes, characterized by having unpaired

Received: March 28, 2025
Revised: April 22, 2025
Accepted: April 25, 2025
Published: May 8, 2025

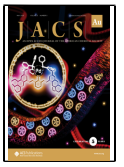

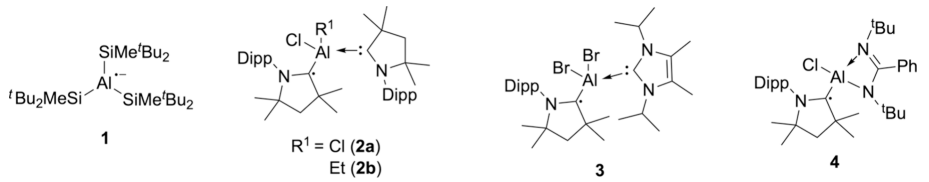

Figure 1. Mononuclear aluminum radicals that are amenable to isolation.

Scheme 1. Dimerization and Solvent Reduction by a Putative Al(II) Intermediate

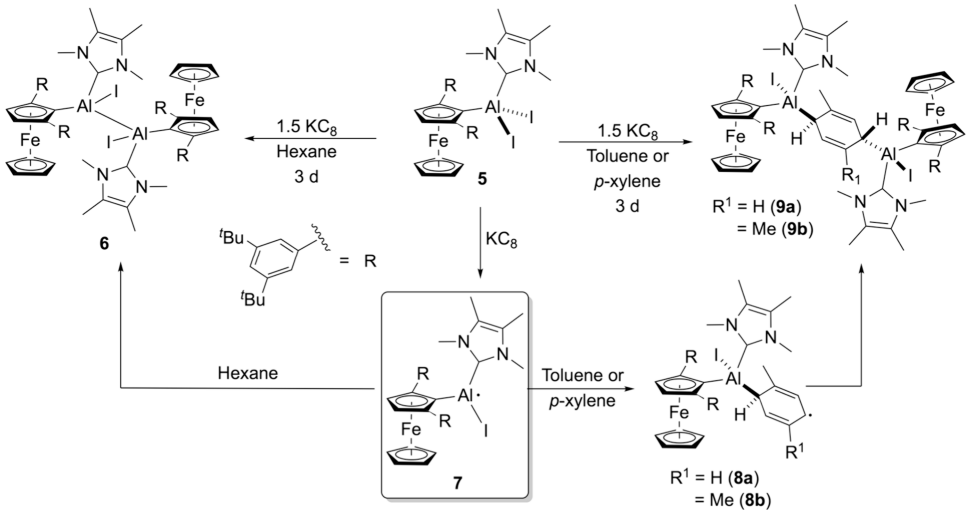

electrons, tend to be highly unstable and often dimerize by Al−Al bond formation. Consequently, developing metastable, mononuclear Al(II) compounds for small molecule activation would be beneficial and offer complementary behavior to the polar reaction pathways of the more explored Al(III) and Al(I) ions.

This Perspective provides an overview of the radical chemistry of mononuclear aluminum complexes, focusing on their reactivity toward small molecules. We begin by discussing isolable mononuclear aluminum radicals, including cases both with aluminum-centered spin and with stabilization from redox non-innocent ligands. Then, we explore how aluminum radicals have been successfully employed in Birch-type reductions via outer-sphere electron transfer mechanisms. Next, we discuss strategies for generating Al radical intermediates under mild conditions, such as Al-M hetero-bimetallic homolysis and photolysis. Finally, we provide meta-analyses of the mononuclear Al radical chemistry literature, covering (a) molecular design features that enable inner-sphere small molecule activation through biphilic character at aluminum and (b) emerging analogies between reaction chemistries of Al radicals and those of *d*-and *f*-block metal ions such as Ti(III) and Sm(II), respectively.

Understanding and controlling the chemistry of the underexplored oxidation state, Al(II), of earth's most abundant metal can unlock new strategies for bond activation, catalysis, and material development. We hope that the fundamental molecular design concepts highlighted in this Perspective provide bridges to such emerging and versatile use cases in the near future.

ISOLABLE ALUMINUM RADICALS

The first isolable aluminum radicals reported in the literature were dialane radical anions prepared by the groups of Power and Pörschke, respectively, in 1993.[16,17] To isolate the first mononuclear Al(II) species, Sekiguchi and co-workers turned to a strategy they had previously used to isolate heavy Group 14 radicals with bulky di-*tert*-butylmethylsilyl (^{t}Bu$_2$MeSi) stabilization.[18] In 2005, they successfully used the ^{t}Bu$_2$MeSi group to stabilize a tris(di-*tert*-butylmethylsilyl)aluminum radical anion (**1**, Figure 1) by alkali metal reduction of the neutral alane, (^{t}Bu$_2$MeSi)$_3$Al.[19] Complex **1** was the first isolated complex in which an unpaired electron was situated on a single Al atom, as fully characterized by X-ray crystallography and EPR spectroscopy. One-electron oxidation of **1** with [Ph$_3$C][B(C$_6$F$_5$)$_4$] regenerated the (^{t}Bu$_2$MeSi)$_3$Al precursor.

In several instances, cyclic (alkyl)(amino)carbene (cAAC) ligands have been used to stabilize Al radicals. Reduction of (cAAC)AlCl$_3$, (cAAC)AlEtCl$_2$, and (cAAC)AlBr$_3$ compounds with KC$_8$ in the presence of exogenous cAAC or NHC ligands has enabled isolation of compounds **2a**, **2b**, and **3** (Figure 1).[20−22] Similarly, reduction of LAlCl$_2$ with KC$_8$ in the presence of cAAC afforded the radical LAlCl(cAAC) (**4**, L = PhC(N^{t}Bu)$_2$).[23] One electron oxidation of **3** by [Ph$_3$C][B(C$_6$F$_5$)] was found to give [(cAAC)AlBr$_2$(IPr)][B(C$_6$F$_5$)$_4$], a rare example of a carbene-stabilized Al cation.[20] Theoretical investigations of **2a**, **2b**, **3**, and **4** revealed that, in each case, the unpaired electron is predominantly localized on carbene carbon atoms rather than aluminum, as corroborated by EPR measurements. In other words, these formally Al(II) complexes are best viewed as Al(III) coordinated to carbene radical anions.

ALUMINUM-PROMOTED BIRCH REDUCTION

Although seminal work by the groups of Fedushkin[24−26] and Braunschweig/Fantuzzi[27] demonstrated small activation by

https://doi.org/10.1021/jacsau.5c00352
JACS Au 2025, 5, 2076−2088

Scheme 2. Reactivity of a Spectroscopically Observed Al(II) Intermediate

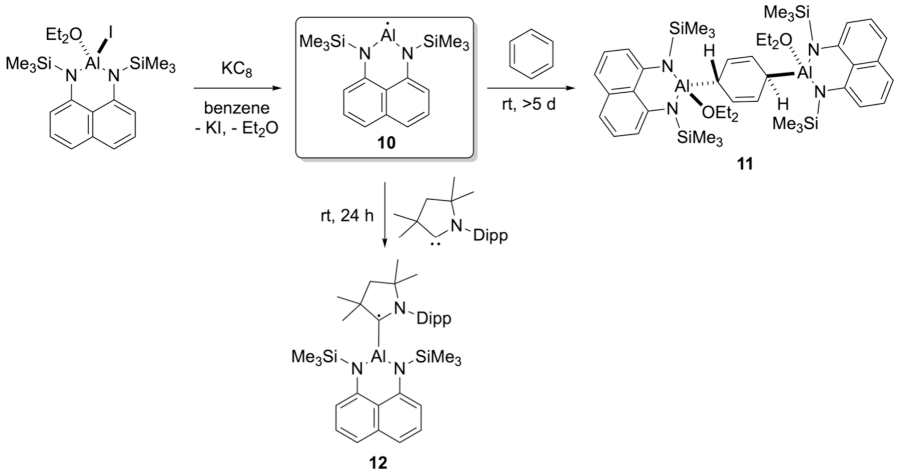

Scheme 3. Radical Pair Reactivity Involving a Redox Non-innocent Al Radical

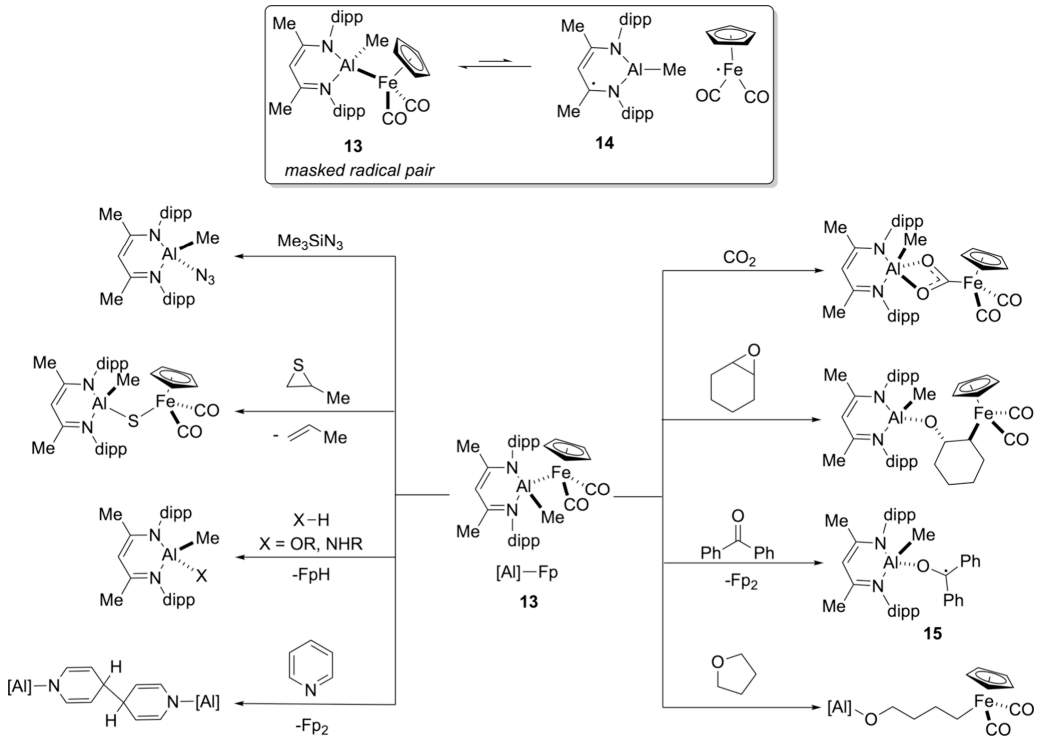

redox non-innocent dialuminum radicals, reaction chemistry of mononuclear Al radicals has only emerged in recent years.

In 2022, Braunschweig and co-workers introduced redox-active (ferrocenyl)aluminum compound **5** (Scheme 1).[28] In hexane, one-electron reduction with KC_8 produced dialane **6**, while two-electron reduction resulted in products from C–H activation of the *N*-heterocyclic carbene. In aromatic solvents, one-electron reduction led to solvent activation, i.e., a dialuminyl Birch reduction. DFT calculations indicated that both the dialane and arene reduction products originate from the initial formation of a base-stabilized Al(II) radical **7**, which undergoes radical homocoupling in hexane to give **6** or electron transfer to an arene solvent to yield intermediates **8a**,**b** and, ultimately, products **9a**,**b**. In this case, radical intermediate **7** was not detected directly.

In 2023, Andrada and Kay developed an aluminum system with a rigid supporting scaffold and bulky silyl protecting groups.[29] Reduction of the corresponding aluminum(III) iodide complex was proposed to form an Al(II) radical intermediate (**10**, Scheme 2) that proceeds to a Birch reduction product of benzene (**11**). Low-temperature EPR monitoring along with DFT calculations provided evidence for Al(II) intermediate **10**. In particular, the EPR spectrum of **10** showed a six-line pattern consistent with coupling to ^{27}Al (100% natural abundance, $I = 5/2$). Accordingly, spin density calculations indicated that the unpaired electron is localized at the aluminum center with small contributions from the nitrogen atoms of the supporting ligand. All attempts to isolate the Al(II) species **10** were unsuccessful. Nonetheless, this finding represents the first direct detection of a mononuclear Al(II) intermediate relevant to small molecule

https://doi.org/10.1021/jacsau.5c00352
JACS Au 2025, 5, 2076–2088

Scheme 4. Multisite, Asynchronous Proton-Coupled Electron Transfer Mechanism Involving Coordination-Induced Bond Weakening of H_2O by an Al Radical

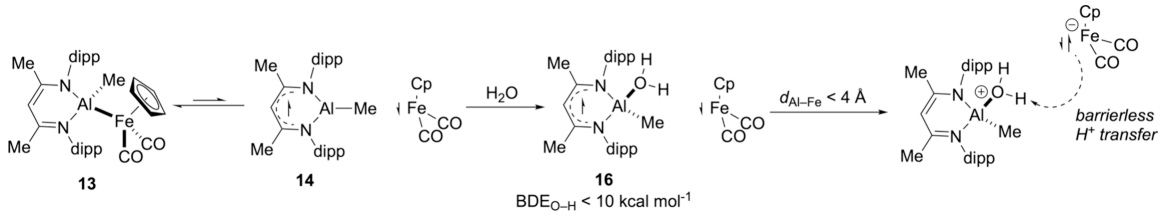

Scheme 5. Regioselective Epoxide Opening as a Mechanistic Probe

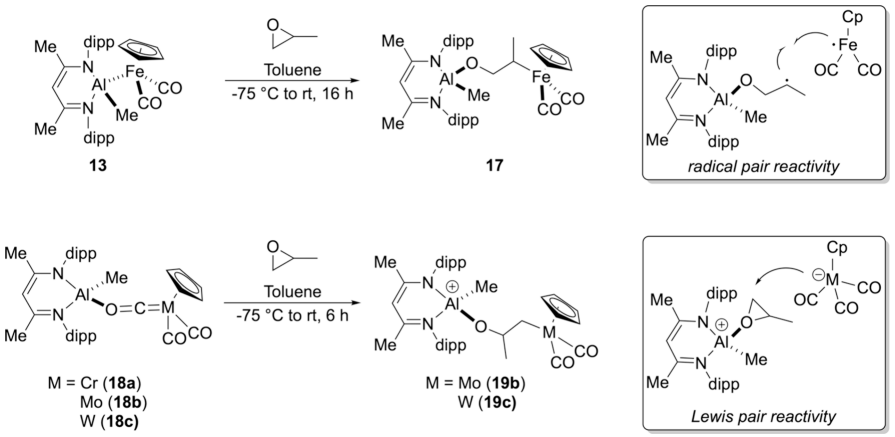

activation. In a trapping experiment, conducting the KC_8 reduction in the presence of cAAC in benzene produced deep yellow **12**, in which the cAAC ligand is redox non-innocent akin to **2**, **3**, and **4** discussed above.

ALUMINUM RADICALS FROM HETEROBIMETALLIC PRECURSORS

The preceding examples are proposed to involve mononuclear Al(II), but the ability to study the reaction chemistry was limited by the harsh conditions (i.e., KC_8 reduction) required for accessing the reactive intermediates. Recently, cases have emerged in which Al radical intermediates were accessed under milder conditions enabled by Al−M homolysis, thus allowing for expansion of the known reaction chemistry of mononuclear Al-containing radicals.

In 2022, our group discovered that the heterobinuclear complex LAl(Me)Fp (**13**, L = $[HC(CMeNdipp)_2]^-$, dipp = 2,6-di-*iso*-propylphenyl, Fp = $[FeCp(CO)_2]^-$) has an unusually weak Al−Fe bond, causing it to dissociate homolytically under ambient conditions to equilibrate with its radical pair form that includes Al-containing radical **14** (Scheme 3).[30] Due to the equilibrium lying toward the Al−Fe side, intermediate **14** was not detected directly. However, electronic structure calculations indicated that **14** is best considered to be an Al(III) complex supported by the radical dianionic form of the *β*-diketiminate. No spin density was apparent at the Al center computationally, and the calculations indicate significant lengthening of the C−N bonds upon Al−Fe cleavage. Thus, key intermediate **14** is biphilic, possessing both an electrophilic Al(III) center and a reducing ligand radical. This bifunctionality leads to high reactivity, and complex **13** was found to activate (via intermediate **14**) CO_2, epoxides, THF, propylene sulfide Me_3SiN_3, benzophenone, and pyridine, giving rise to the range of products shown in Scheme 3.[30−32] In all cases, it is proposed that the coordination of heteroatoms to the Al(III) center in **14** induces either *σ*-bond weakening or reduction of a *π*-system. The most direct evidence of the intermediacy of **14** comes from trapping it with benzophenone to afford a new radical, LAl(Me)($OCPh_2$) (**15**), that was characterized by EPR and electron nuclear double resonance (ENDOR) spectroscopies. Compound **15** was determined to contain the closed-shell (monoanionic) form of the *β*-diketiminate and a reduced benzophenone ketyl radical coordinated to Al(III).

Complex **13** reacts rapidly with O−H substrates (H_2O, MeOH, *i*PrOH, ^{t}BuOH) and an N−H substrate (^{i}BuNH$_2$) at temperatures as low as −30 °C, providing FpH and LAl(Me)X as the products (X = OH, OMe, O^{i}Pr, O^{t}Bu, NH^{i}Bu).[32] This reactivity is thought to be associated with the formation of the **14**/Fp radical pair. Notably, studies in 2024 demonstrated that X−H activation processes involving these species can proceed via proton-coupled electron transfer (PCET) mechanisms. Accordingly, the rate of X−H activation was unaffected by the pK_a of the substrate. No kinetic isotope effect was observed when comparing rates of MeOH vs MeOD activation, consistent with Al−Fe cleavage of **13** being rate determining and substrate coordination and activation occurring after the rate-limiting step. Computational modeling of the H−OH activation mechanism indicated an asynchronous PCET process in which the LAl(Me)(OH_2) radical (**16**) first transfers an electron from the reduced *β*-diketiminate to Fp·, followed by barrierless H^+ transfer between the incipient $[LAl(Me)(OH_2)]^+[Fp]^-$ ion pair (Scheme 4). Because the H^+ and e^- equivalents being transferred during PCET are not colocalized in **16**, this reaction can be considered an example of multisite PCET.[33] Notably, coordination induced bond weakening (CIBW) of H_2O upon interacting with radical intermediate **14** is quite dramatic, with the aquo adduct **16** calculated to have a O−H bond dissociation enthalpy of <10 kcal mol^{-1}.[32]

https://doi.org/10.1021/jacsau.5c00352
JACS Au 2025, 5, 2076−2088

This degree of CIBW is on par with the most dramatic examples in the literature involving divalent *f*-elements.[34,35]

Further evidence for the intermediacy of radical **14** came from comparing reaction chemistry toward (±)-propylene oxide of Al/Fe complex **13** and its Al/M analogues with those of Group VI transition metals. The complexes LAl(Me)[MCp-$(CO)_3$] (M = Cr, **18a**; Mo, **18b**; W, **18c**) were synthesized by reacting Na[CpM$(CO)_3$] precursors with LAl(Me)I. These Al/M structures were found to be end-on "isocarbonyl" type Al—O═C═M compounds with metalloketene character rather than having direct metal−metal bonds like the Al−Fe bonded **13**.[32,36] Regioselective ring opening of (±)-propylene oxide was observed for complexes **13**, **18b**, and **18c**, with **13** giving rise to product **17** with a secondary Fe−C bond and **18b,c** giving rise to products **19b,c** with primary M−C bonds (Scheme 5). The opposing regioselectivity was attributed to **13** behaving as a masked radical pair (i.e., **14** + Fp·) and the Group VI analogues behaving as masked Lewis pairs (i.e., $[LAlMe]^+[MCp(CO)_3]^-$). As such, the results can be interpreted as CIBW of (±)-propylene oxide by **14** resulting in C−O cleavage to place the radical on the more substituted side of the epoxide, compared to Lewis acid activation of the epoxide by **18b,c** occurring at the less hindered side of the epoxide as expected for S_N2-type pathways.[37]

Although the preceding experiments implied that the **18** series behaves as masked Lewis pairs, further computational and experimental studies in 2024 showed that these compounds can access both Lewis pair and radical pair manifolds depending on reaction conditions.[36] For example, double crossover experiments indicated equilibration between the **18** complexes and the masked radical pair **13**, hinting that the **18** derivatives generate radical intermediates under these conditions. Indeed, computational modeling indicated that the $[LAlMe]^+[MCp(CO)_3]^-$ ion pairs and $[LAlMe]^{\cdot}[MCp(CO)_3]^{\cdot}$ radical pairs tend to be close in energy for the Group VI triad. Assuming thermal equilibration between the ionic and radical pair forms, photochemical conditions favor the radical pair form of **18a**, enabling it to mimic the thermal reactivity of **13**. (Scheme 6a). Photolysis of **18a** in the presence of benzophenone produced **15** that had previously been characterized during studies of **13**.[30] Additionally, photolysis of **18a** resulted in reductive decarbonylation of the $CpCr(CO)_3$ fragment, producing tetrametallic Al_2Cr_2 species **20**.[36] An analogous Al_2Fe_2 product had been previously reported upon photolysis of **13**,[31] further underlining the radical pair nature of **18a** under photochemical conditions. Photolysis of a putative $LAl(Me)Mn(CO)_5$ species generated *in situ* also produced reductive decarbonylation product **21** containing an Al_2Mn_2 core (Scheme 6b).[36]

To further understand the ability to unmask mononuclear Al radicals from Al−M bonds, our group has reported data-intensive computational studies probing both ligand effects on and periodic trends in Al−M bond strengths.[38,39] Although the details will not be reviewed here comprehensively, in short, many of the observed trends can be traced to electronic and steric stabilization of the Al radicals generated upon Al−M homolysis.

In 2024, Aldridge and co-workers studied the bis(aluminyl)-magnesium complex $Mg[Al(NON)]_2$ (**22**) and found it to be a source of nucleophilic $[Al(NON)]^-$ under thermal conditions and radical $[Al(NON)]^{\bullet}$ (**23**) under photochemical conditions. Photolysis of a benzene solution of **22** in the presence of 1,5-cyclooctadiene resulted in transannular cycloaddition

Scheme 6. Light-Induced Radical Chemistry of Al/Cr and Al/Mn Complexes

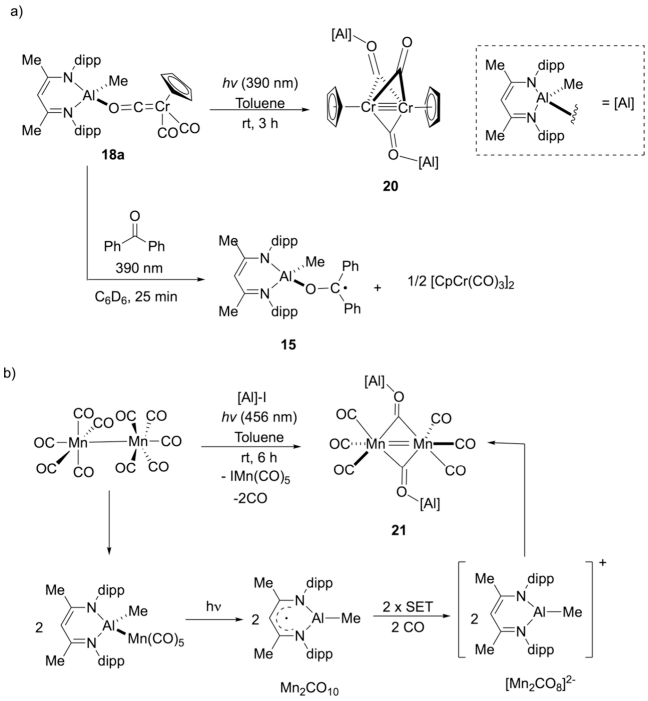

product **24** (Scheme 7).[40] In the absence of 1,5-cyclooctadiene, photolysis of **22** in hexane produced (NON)Al−Al(NON) (**25**) and magnesium metal. The aluminum-centered radical **23** was proposed as the key intermediate in these transformations. Evidence for the intermediacy of **23** was obtained from EPR monitoring of the photolysis, and observation of significant coupling to ^{27}Al provided evidence for the Al(II) assignment. However, further elucidation of the electronic structure of **23** was not reported until work by our group.

Our group in collaboration with Ess and co-workers recently revisited the Al−Fe cleavage chemistry discovered for **13**, but now using (NON)Al−Fp (**26**) as a masked radical pair.[41] Since homolytic cleavage of **13** resulted in intermediate **14** with a reduced *β*-diketiminate, we hypothesized that replacing monoanionic *β*-diketiminate with dianionic $(NON)^{2-}$ would make ligand reduction less likely and, therefore, favor localization of spin density at the Al center (as indicated by the work of Aldridge,[40] see above). Accordingly, in addition to carboxylation by CO_2 gas yielding **27** as previously known for **13**, the addition of TEMPO (2,2,6,6-tetramethyl-1-piperidinyloxy) as a radical scavenger to **26** led to stoichiometric formation of Fp_2 and (NON)Al(TEMPO) (**28**, Scheme 8). Similarly, addition of benzophenone to **26** resulted in stoichiometric formation of Fp_2 and trapped the Al radical as $(NON)Al(OCPh_2)$ (**29**), which like **15** was characterized by EPR spectroscopy.

Carboxylation of the Al−Fe bond in **26** was subjected to a mechanistic investigation. Combining experimental and theoretical results, a radical pair mechanism was proposed by which the homolytic cleavage of **26** leads to Al(NON) (**23**), the same radical intermediate previously proposed by Aldridge.[40] Computational modeling of **23** indicated that the spin density is Al-centered; i.e., **23** is a mononuclear Al(II) intermediate. Additionally, frontier orbital analysis of **23**

https://doi.org/10.1021/jacsau.5c00352
JACS Au 2025, 5, 2076−2088

Scheme 7. Access to a Mononuclear Al(II) Intermediate by Photolytic Al−Mg Cleavage

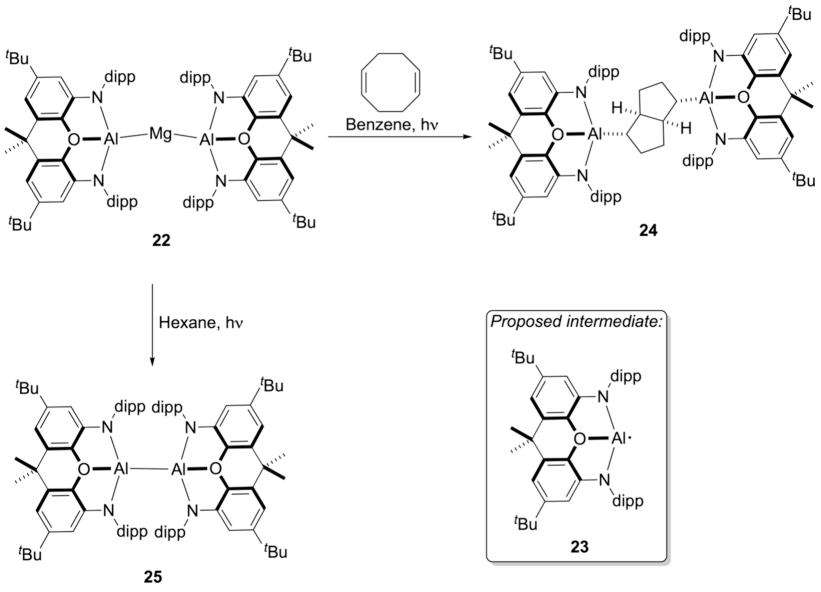

Scheme 8. Reactivity of an Al−Fe Complex Lacking Ligand-Based Redox Activity toward CO_2 and Radical Scavengers

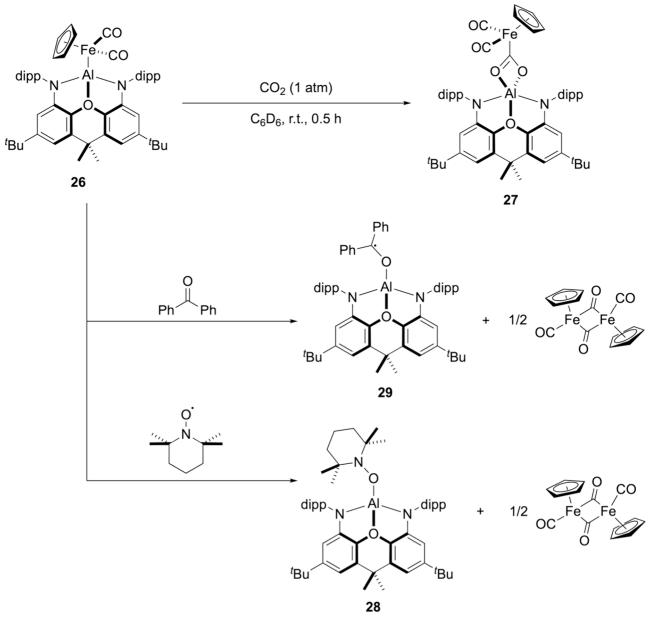

indicated a small SOMO/LUMO gap resulting from the strained geometry enforced by the NON chelate,[42] as will be discussed in detail below. As such, the Al(II) center in **23** can be considered biphilic in that it is simultaneously Lewis acidic and reducing. This biphilicity enables coordination and the subsequent activation of CO_2. In the computed reaction pathway (Scheme 9), initial coordination of CO_2 to the Al center in **23** is followed by charge transfer from Al(II) to the CO_2 ligand, resulting in intermediate **30** that is best considered as containing a $[CO_2]^{\bullet-}$ ligand bound to Al(III). Finally, barrierless radical coupling with Fp· provides the final metallocarboxylate **27**.

PHOTOCHEMISTRY AND PHOTOCATALYSIS

Homolysis of compounds with heavy *p*-block elements like tin and bismuth is enabled by their relatively low homolytic bond dissociation energies and their energetically accessible charge-transfer excited states.[43−46] Analogous chemistry with lighter *p*-block elements like Al often requires introduction of non-innocent ligands to produce low lying acceptor orbitals accessible by visible light irradiation. For example, aluminum complexes of pyrazine or bipyridine readily undergo thermal or photochemical radical formation.[47] Similarly, aluminum porphyrins are stable precursors at ambient conditions but exhibit photoreactivity when exposed to light.[48] In 2024, Breher, Unterreiner, and co-workers developed bis-(pyridylimino)isoindolide aluminum complexes **31** (Scheme 10) that exhibit efficient charge transfer homolysis upon visible-light excitation, making them a convenient platform for generating carbon-centered radicals.[49] Evidence of methyl radical generation was obtained from radical trapping experiments with TEMPO and 5,5-dimethyl-pyrroline N-oxide (DMPO) as well as other experimental and computational methods. In the absence of any radical trap, methylation of the isoindolide to generate complex **32** was observed. This charge transfer homolysis behavior was exploited to develop Sn-free Giese-type conjugate additions (Scheme 10), C═O alkylations, and C−C coupling applications under ambient conditions.

In 2023, Gilmour, Neugebauer, and co-workers developed photocatalytic (400 nm, violet light) deracemization of cyclopropyl ketones, achieving up to 98:2 enantiomeric ratio using the chiral Al(salen) complex (*R*,*R*)-**33** as the catalyst (Scheme 11).[50] Catalytic activation of cyclopropyl ketones is otherwise typically achieved by transition metal catalysis involving, for example, Ru, Ni, or Ti.[51−53] The proposed mechanism for the Al-catalyzed transformation involves both Lewis acid activation and light-induced single electron transfer to the cyclopropyl ketone substrate. As such, this study provides another example leveraging the biphilic behavior of an aluminum radical intermediate.

WHAT ENABLES BIPHILICITY?

The evolution of the mononuclear Al radical design is evident from the preceding sections (Scheme 12). For complex **1**, the first mononuclear Al(II) species to be isolated, only outer-

https://doi.org/10.1021/jacsau.5c00352
JACS Au 2025, 5, 2076−2088

Scheme 9. Radical Pair Mechanism for Al−Fe Carboxylation

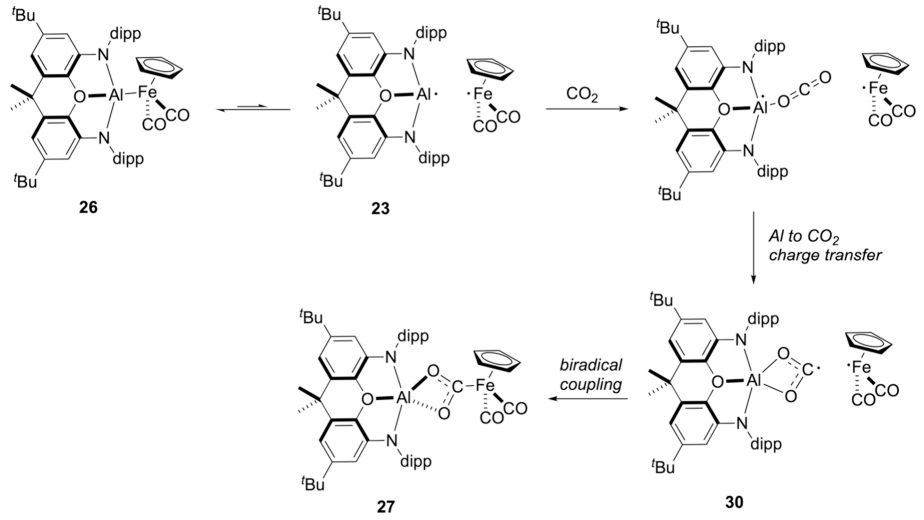

Scheme 10. Photochemical Reactivity and Sn-Free Giese Behavior of a Redox Non-innocent Aluminum System

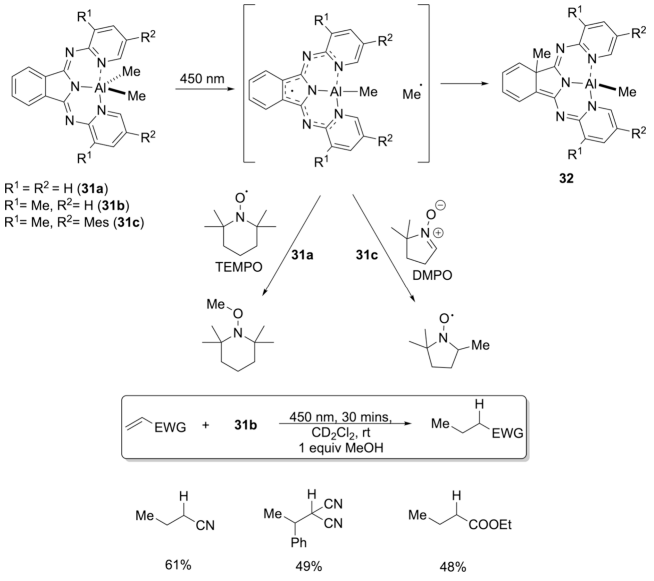

sphere electron transfer chemistry was reported.[18] Presumably, this is because the trigonal planar Al center in **1** has 7 valence electrons and, thus, lacks the Lewis acidity needed to bring substrates into the Al coordination sphere. The same logic applies to other Al(II) intermediates such as radical **7** that are known to perform Birch reduction in analogy to metallic Na but were not observed to engage in any inner-sphere reaction chemistry.[28]

Inner-sphere reaction chemistry became possible when biphilic Al radicals were accessed by using one of two strategies. In the first strategy (Scheme 12, left), intermediate **14** exhibits biphilicity despite maintaining a trigonal planar coordination environment due to the redox non-innocence of the supporting ligand.[30] The Al center in **14** is a 6-electron Al(III) site and, thus, possesses a vacant *p*-orbital for substrate coordination. Upon substrates entering the Al coordination sphere, they are placed in proximity to the reducing ligand radical and undergo activation via coordination-induced weakening.[32]

In the second strategy (Scheme 12, right), intermediate **23** exhibits biphilicity despite having a redox innocent ligand due to the strained Al geometry. Strain-induced biphilicity is an emerging theme in *p*-block chemistry.[42,54−58] In this case, the descent in symmetry from trigonal planar (C_{3v}) to approximately T-shaped (C_{2v}) lowers the SOMO/LUMO gap significantly.[41] (Intermediate **23** is descended further to C_s symmetry characterized by a bent geometry at the Al−O axis.) In this regime, the Al-centered LUMO is energetically accessible for nucleophilic attack despite the 7-electron valence count.

Although the electronic structure of strained intermediate **23** was detailed in our previous work,[41] here, we provide a more general Walsh-type correlation diagram[59] using density functional theory (DFT) analysis of the simple Al(II) species, $[AlH_3]^-$ (Figure 2). In 3-fold symmetry (C_{3v}), the singly occupied molecular orbital (SOMO) is $2a_1$, while the doubly degenerate 2e orbitals represent the lowest unoccupied molecular orbital (LUMO) set. The energy difference between the SOMO and LUMO levels in this ground-state configuration is 121 kcal mol^{-1} (5.25 eV). Upon distortion to C_s symmetry, the SOMO remains largely unchanged, but the degeneracy of the LUMO level is lifted, with the new LUMO being lowered in energy due to decreased destructive overlap between the three H atoms and $3p_x$. Consequently, the SOMO-LUMO energy gap becomes 111 kcal mol^{-1} (4.81 eV), around 10 kcal mol^{-1} (0.44 eV) lower than that in the C_{3v} ground state. Further distortion to a C_{2v}-symmetric, T-shaped structure accentuates these effects and leads to strictly orthogonal SOMO and LUMO wave functions. At the T-shaped structure, the SOMO-LUMO gap is drastically decreased to 46 kcal mol^{-1} (1.99 eV), which is 75 kcal mol^{-1} (3.26 eV) lower than in the C_{3v} case. Thus, a T-shaped Al(II) species can safely be considered biphilic since it would simultaneously carry a high-energy unpaired electron and a low-lying electrophilic molecular orbital. Interestingly, the frontier orbitals for **23** are inverted compared to $[AlH_3]^-$, such that the unpaired electron is predicted to be in the σ-type MO for the former but in the π-type MO for the latter.

https://doi.org/10.1021/jacsau.5c00352
JACS Au 2025, 5, 2076−2088

Scheme 11. Photocatalytic Deracemization of Cyclopropyl Ketones by a Redox Non-innocent Al(Salen) Catalyst

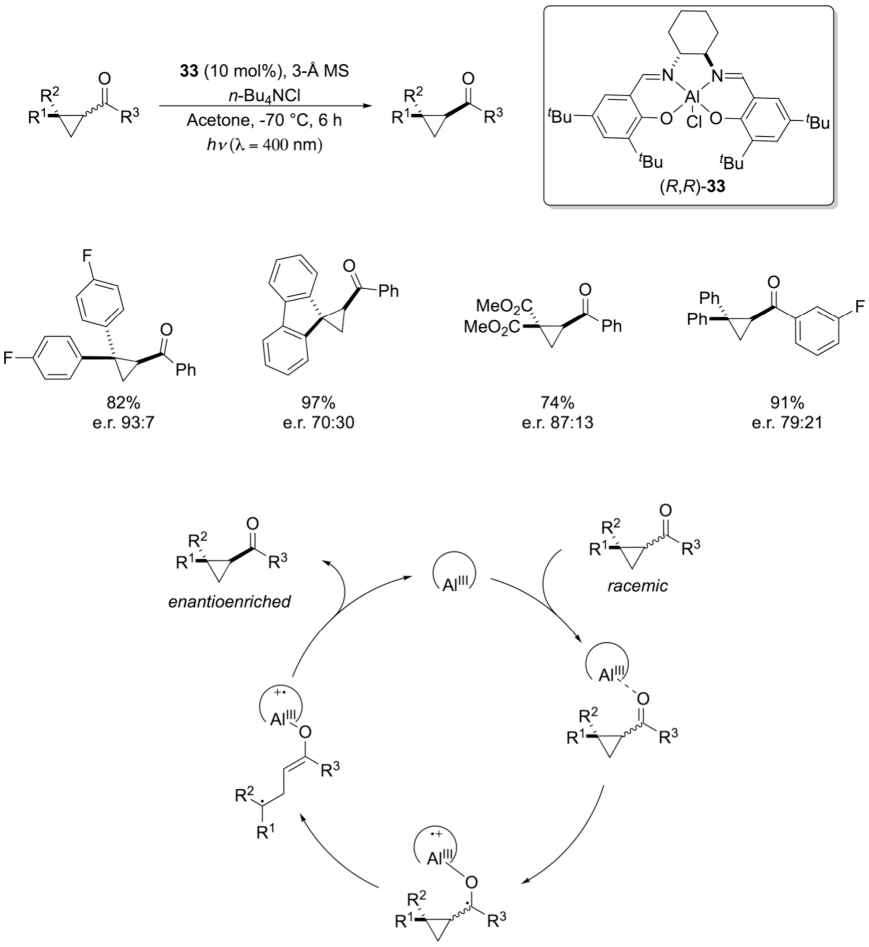

Scheme 12. Strategies for Introducing Biphilicity to Mononuclear Al Radicals

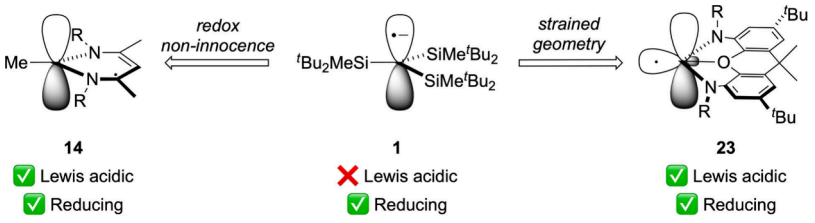

ANALOGIES TO TRANSITION METALS AND LANTHANIDES

Once biphilicity is imparted to mononuclear Al radicals, their reaction chemistry parallels those of certain elements of the *d*- and *f*-blocks of the periodic table. Here, we highlight parallels between the chemistry of mononuclear Al radicals and the behaviors of Ti(III) complexes and divalent *f*-block metals. Interestingly, aluminum and titanium are isodiagonal,[60] and the catalytic results of Gilmour, Neugebauer, and co-workers (Scheme 11)[50] resemble behavior of Ti catalysts.[51]

One aspect of Ti(III) chemistry that is recapitulated in the behavior of Al radicals like **14** is coordination-induced bond weakening (CIBW).[61] Whereas protic ligands such as H_2O or NH_3 undergo acidification in Werner-type coordination complexes, they typically maintain high bond dissociation free energies (BDFEs); i.e., they serve as sources of H^+ but not $H^\bullet$. For certain coordination complexes, however, CIBW results in a dramatic decrease of the X−H BDFE. This CIBW behavior is typically observed for low-valent metals like Mo(I)[62] that are biphilic, maintaining Lewis acidity for substrate coordination while showing strong reducing potential to promote net $H^\bullet$ loss by proton-coupled electron transfer (PCET).[33] A canonical metal ion for which CIBW is well-known is Ti(III). For example, whereas the $BDFE_{O-H}$ of H_2O is 113 kcal mol^{-1},[33] the aquotitanium(III) complex, $Cp_2TiCl(OH_2)$ (**34**), has a $BDFE_{O-H}$ of 49 kcal mol^{-1} due to CIBW (Scheme 13).[63] Similarly, addition of H_2O to Al−Fe compound **13** produces intermediate **16**, which was calculated to have a $BDFE_{O-H}$ of ∼1 kcal mol^{-1},[32] rivaling the most dramatic examples of CIBW that were discovered in the *f*-block (see below). Although the net reaction chemistries of **16** and **34** are analogous, there are important differences to note. In the case of **34**, the Lewis acid and electron donor sites are colocalized at the Ti(III) ion. On the other hand, redox non-innocent **16** spatially separates the Lewis acidity at the Al(III) site from the electron donor stored in the ligand backbone.

https://doi.org/10.1021/jacsau.5c00352
JACS Au 2025, 5, 2076−2088

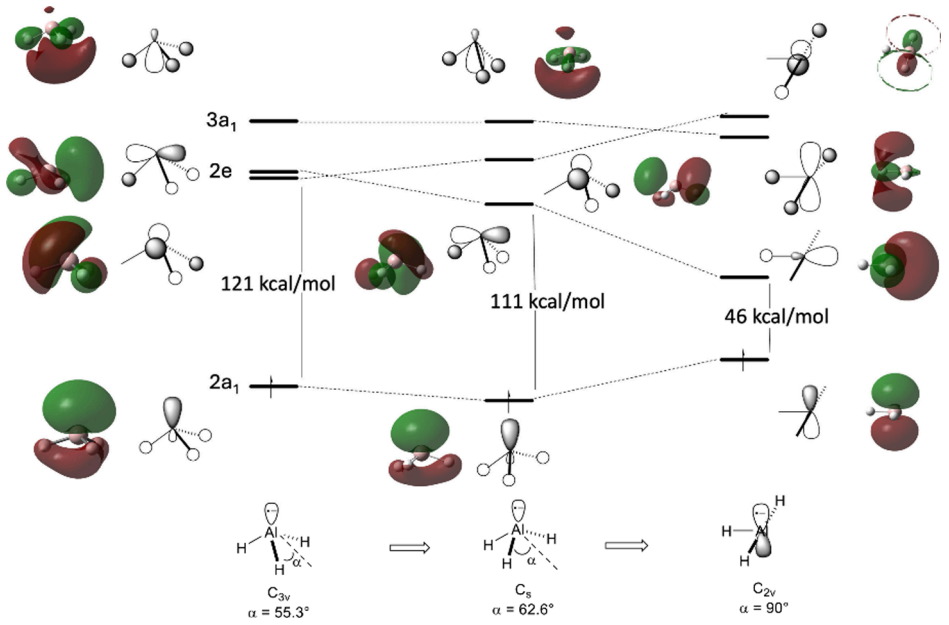

Figure 2. Frontier molecular orbital correlation diagram for $[AlH_3]^-$ calculated at the B3LYP-D3BJ/6-31G(d) level of DFT.

Scheme 13. Examples of the Ti(III)/Al(II) Analogy

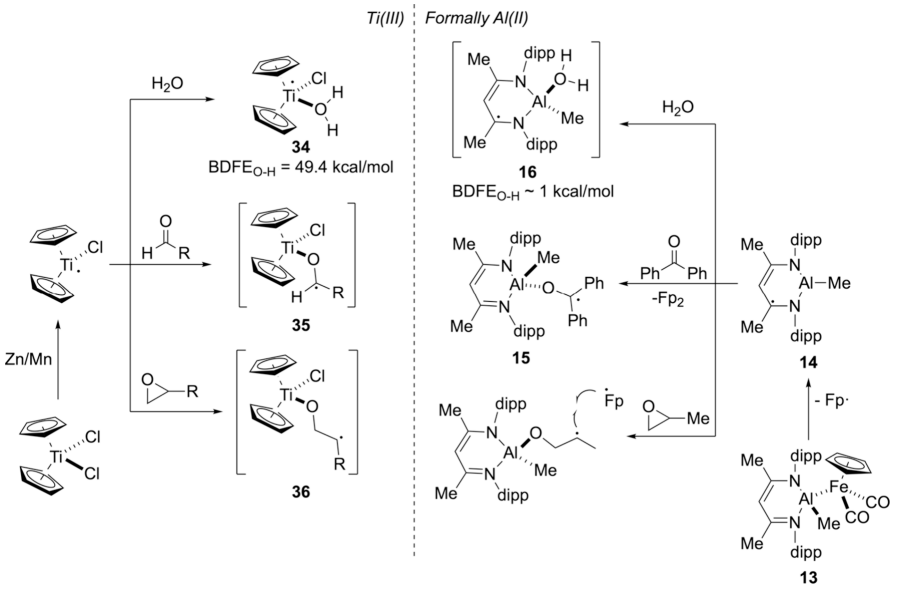

Scheme 14. Examples of the Sm(II)/Al(II) Analogy

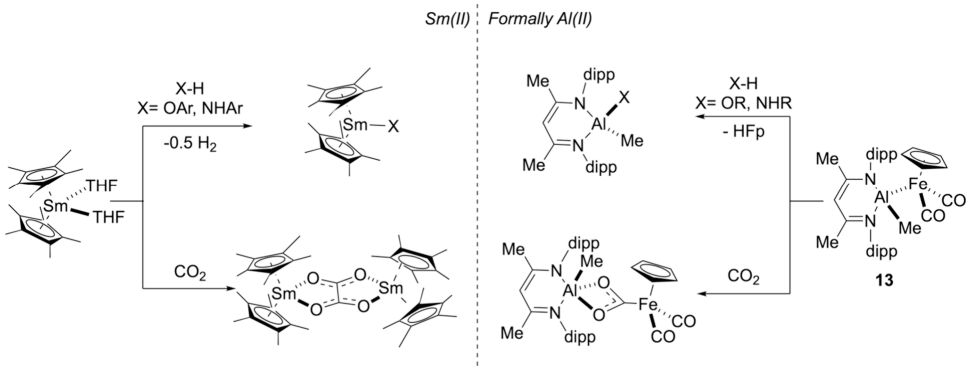

https://doi.org/10.1021/jacsau.5c00352
JACS Au 2025, 5, 2076−2088

Further parallels between Al radicals and Ti(III) compounds emerge from the activation of C−O and C═O bonds. For example, generation of the [Cp_2TiCl] intermediate in the presence of aldehydes or epoxides are well-known to generate carbon-centered radical species **35** and **36**, respectively (Scheme 13), that can be intercepted for productive synthesis.[64,65] In the case of epoxides, Ti(III)-induced ring opening tends to occur with regioselectivity that generates the more substituted (and thus more stable) carbon radical. Similar reactivity was observed for intermediate **14**, which was trapped by benzophenone to produce ketyl radical species **15** and by (±)-propylene oxide to produce the ring opening product with Ti(III)-like regioselectivity.[30,32]

Due to the supply risk and environmental impact associated with rare-earth metals, mimicking *f*-element properties with aluminum offers a more sustainable approach to small-molecule activation.[66,67] One of the most active areas of research in *f*-element chemistry has been to study divalent lanthanide ions such as Sm(II), including solubilized forms like $SmCp^*_2$, for their unique small molecule activation chemistry enabled by potent Lewis acidity combined with strong reducing potential.[68] As discussed previously for Ti(III), one parallel between Sm(II) and Al radicals is the ability to engage in the CIBW of X−H substrates. For example, aqueous SmI_2 and $SmBr_2$ produce substantial weakening of the O−H bond of water by approximately 74 kcal mol^{-1} and 83 kcal mol^{-1} respectively,[69] similar to the ∼112 kcal mol^{-1} bond weakening of H_2O determined for intermediate **16**.[32] Accordingly, exposure of $Cp^*_2Sm(THF)_2$ to phenols or anilines (Scheme 14) results in formation of Sm(III)−O or Sm(III)−N bonds with the evolution of H_2 gas (presumably via dimerization of $H^•$).[70,71] This behavior bears similarities to the behavior of masked aluminum radical **13**, which reacts with alcohols and amines to form Al(III)−O and Al(III)−N bonds with loss of H-Fp (via net $H^•$ transfer).[32] Consistent with the CIBW effect being even stronger for the Al radical system than for Sm(II), aliphatic amines undergo $H^•$ loss when added to **13** but simply form adducts with $Cp^*_2Sm(THF)_2$.[72]

A signature reaction of Sm(II) is reductive coupling of CO_2 to form oxalate (Scheme 14),[73] a reaction that is presumed to occur via coupling of two $[CO_2]^{•-}$ ligands. Analogously, exposure of masked Al radicals **13** and **26** to CO_2 produces metallocarboxylate compounds by mechanisms proposed to involve $[CO_2]^{•-}$ ligands bound to Al(III).[30,41] The fact that oxalate formation was not observed in the Al−Fe cases implies that Fe−C formation by the rebound of $Fp^•$ to the $[CO_2]^{•-}$ ligand occurs at a faster rate than dimerization under the conditions examined. These observations raise the possibility that oxalate formation from Al radicals could be achievable under alternative reaction conditions, although CO_2 coupling remains a complex transformation that is highly sensitive to geometric, electronic, and ligand effects.

Two additional parallels between the divalent lanthanide reactivity and Al radical reactivity are shown in Figure 3. First, trapping of Al radical **14** by pyridine results in bipyridyl radical coupling and formation of a dialuminum(III) 1,1′-bis(1,4-dihydropyridylamide) species.[32] A similar reaction occurs between pyridine and [$(1,2,4\text{-}C_5H_2{}^tBu_3)_2Tm$], also providing a bridging bis(1,4-dihydropyridylamide) ligand via coupling of two pyridine radicals.[74]

Second, reductive decarbonylation products **20** and **21** contain unsaturated metal carbonyl dimers $[(CpCr)_2(CO)_3]^{2-}$ and $[Mn_2(CO)_8]^{2-}$, resulting from the activity of photochemically generated Al radicals on parent compounds such as $Mn_2(CO)_{10}$ (e.g., see Scheme 6).[36] Analogous reduction of $Re_2(CO)_{10}$ and $Co_2(CO)_8$ by different divalent lanthanides has also been reported to yield products with, e.g., $[Re_2(CO)_8]^{2-}$ cores (Figure 3),[75,76] further highlighting the similar reactivity of Al radicals and divalent lanthanide ions.

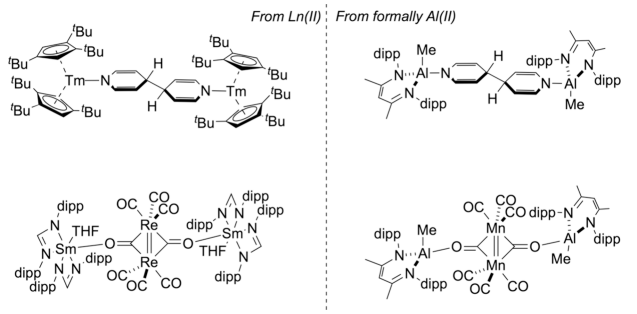

Figure 3. Products demonstrating the analogy between Al radicals and divalent lanthanides.

CONCLUSIONS

Mononuclear Al(II) compounds are challenging to access due to their tendency to dimerize via Al−Al bond formation or to decay via other pathways. However, they can be isolated using bulky supporting groups and/or redox non-innocent ligands. In the latter case, Al(II) compounds are best described as Al(III) compounds with ligand-centered radicals. Strategies such as heterobinuclear Al−M compounds acting as "masked" Al radicals have enabled access to these intermediates under mild conditions, thus facilitating the mapping of diverse reaction pathways. Under certain circumstances such as ligand non-innocence or strained, T-shaped coordination geometries, Al radicals can exhibit biphilic behavior, thus enabling them to mimic the chemistry of *d*- and *f*-block elements that, in some cases, are markedly less earth abundant than aluminum.

Harnessing the reactivity of mononuclear Al radicals will enable the modulation of single-electron chemistry toward small molecules, resembling those of early transition and rare earth metals. Additionally, coupling Al radicals with low-valent transition metals can generate masked radical pairs capable of performing cooperative reactions, resulting in net two-electron processes necessary for cross-coupling and other important applications in catalysis. The molecular design strategies outlined in this Perspective serve as a guide for future systems to access such reaction manifolds.

COMPUTATIONAL DETAILS

Density functional theory (DFT) calculations for $[AlH_3]^-$ were performed using Gaussian 16 (version B.01), employing the B3LYP functional with an ultrafine integration grid and the 6-31G(d) basis set.[77] Empirical dispersion corrections were incorporated using Grimme's D3 empirical dispersion correction, along with the Becke−Johnson (BJ) damping function.[78,79] The SMD model with default parameters for toluene was used to incorporate implicit solvation effects.[80]

AUTHOR INFORMATION

Corresponding Author

Neal P. Mankad − *Department of Chemistry, University of Illinois Chicago, Chicago, Illinois 60607, United States;* orcid.org/0000-0001-6923-5164; Email: npm@uic.edu

https://doi.org/10.1021/jacsau.5c00352
JACS Au 2025, 5, 2076−2088

Author

Roushan Prakash Singh − *Department of Chemistry, University of Illinois Chicago, Chicago, Illinois 60607, United States;* orcid.org/0000-0001-6279-3040

Complete contact information is available at: https://pubs.acs.org/10.1021/jacsau.5c00352

Author Contributions

The manuscript was written through contributions of all authors. All authors have given approval to the final version of the manuscript.

Notes

The authors declare no competing financial interest.

■ ACKNOWLEDGMENTS

This material is based upon work supported by the U.S. Department of Energy, Office of Science, Office of Basic Energy Sciences, under Grant DE-SC0021055. Computational resources and services were provided by the Advanced Cyberinfrastructure for Education and Research (ACER) group at UIC.

■ REFERENCES

(1) Appel, A. M.; Bercaw, J. E.; Bocarsly, A. B.; Dobbek, H.; DuBois, D. L.; Dupuis, M.; Ferry, J. G.; Fujita, E.; Hille, R.; Kenis, P. J. A.; Kerfeld, C. A.; Morris, R. H.; Peden, C. H. F.; Portis, A. R.; Ragsdale, S. W.; Rauchfuss, T. B.; Reek, J. N. H.; Seefeldt, L. C.; Thauer, R. K.; Waldrop, G. L. Frontiers, Opportunities, and Challenges in Biochemical and Chemical Catalysis of CO_2 Fixation. *Chem. Rev.* **2013**, *113* (8), 6621−6658.

(2) Bullock, R. M.; Chen, J. G.; Gagliardi, L.; Chirik, P. J.; Farha, O. K.; Hendon, C. H.; Jones, C. W.; Keith, J. A.; Klosin, J.; Minteer, S. D.; Morris, R. H.; Radosevich, A. T.; Rauchfuss, T. B.; Strotman, N. A.; Vojvodic, A.; Ward, T. R.; Yang, J. Y.; Surendranath, Y. Using Nature's Blueprint to Expand Catalysis with Earth-Abundant Metals. *Science* **2020**, *369*, 769.

(3) Singh, R. P.; Sinhababu, S.; Mankad, N. P. Aluminum-Containing Heterobimetallic Complexes as Versatile Platforms for Homogeneous Catalysis. *ACS Catal.* **2023**, *13* (19), 12519−12542.

(4) Ni, C.; Ma, X.; Yang, Z.; Roesky, H. W. Recent Advances in Aluminum Compounds for Catalysis. *Eur. J. Inorg. Chem.* **2022**, *2022* (10), e202100929.

(5) Nikonov, G. I. New Tricks for an Old Dog: Aluminum Compounds as Catalysts in Reduction Chemistry. *ACS Catal.* **2017**, *7* (10), 7257−7266.

(6) Li, W.; Ma, X.; Walawalkar, M. G.; Yang, Z.; Roesky, H. W. Soluble Aluminum Hydrides Function as Catalysts in Deprotonation, Insertion, and Activation Reactions. *Coord. Chem. Rev.* **2017**, *350*, 14−29.

(7) Mason, M. R. Aluminum-Based Catalysis. In *Encyclopedia of Inorganic and Bioinorganic Chemistry*; John Wiley & Sons, Ltd., 2015; pp 1−22; DOI: 10.1002/9781119951438.eibc2333.

(8) Chen, E. Y.-X.; Marks, T. J. Cocatalysts for Metal-Catalyzed Olefin Polymerization: Activators, Activation Processes, and Structure−Activity Relationships. *Chem. Rev.* **2000**, *100* (4), 1391−1434.

(9) Ogawa, H.; Yang, Z.-K.; Minami, H.; Kojima, K.; Saito, T.; Wang, C.; Uchiyama, M. Revisitation of Organoaluminum Reagents Affords a Versatile Protocol for C−X (X = N, O, F) Bond-Cleavage Cross-Coupling: A Systematic Study. *ACS Catal.* **2017**, *7* (6), 3988−3994.

(10) Minami, H.; Saito, T.; Wang, C.; Uchiyama, M. Organoaluminum-Mediated Direct Cross-Coupling Reactions. *Angew. Chem., Int. Ed.* **2015**, *54* (15), 4665−4668.

(11) Coles, M. P.; Evans, M. J. The Emerging Chemistry of the Aluminyl Anion. *Chem. Commun.* **2023**, *59* (5), 503−519.

(12) Liu, Y.; Li, J.; Ma, X.; Yang, Z.; Roesky, H. W. The Chemistry of Aluminum(I) with β-Diketiminate Ligands and Pentamethylcyclopentadienyl-Substituents: Synthesis, Reactivity and Applications. *Coord. Chem. Rev.* **2018**, *374*, 387−415.

(13) Hicks, J.; Vasko, P.; Goicoechea, J. M.; Aldridge, S. The Aluminyl Anion: A New Generation of Aluminium Nucleophile. *Angew. Chem., Int. Ed.* **2021**, *60* (4), 1702−1713.

(14) Cui, C.; Roesky, H. W.; Schmidt, H.-G.; Noltemeyer, M.; Hao, H.; Cimpoesu, F. Synthesis and Structure of a Monomeric Aluminum(I) Compound [{HC(CMeNAr)$_2$}Al] (Ar = 2,6-$iPr_2C_6H_3$): A Stable Aluminum Analogue of a Carbene. *Angew. Chem., Int. Ed.* **2000**, *39* (23), 4274−4276.

(15) Hicks, J.; Vasko, P.; Goicoechea, J. M.; Aldridge, S. Synthesis, Structure and Reaction Chemistry of a Nucleophilic Aluminyl Anion. *Nature* **2018**, *557* (7703), 92−95.

(16) Wehmschulte, R. J.; Ruhlandt-Senge, K.; Olmstead, M. M.; Hope, H.; Sturgeon, B. E.; Power, P. P. Reduction of a Tetraaryldialane to Generate Aluminum-Aluminum π-Bonding. *Inorg. Chem.* **1993**, *32* (14), 2983−2984.

(17) Pluta, C.; Pörschke, K.-R.; Krüger, C.; Hildenbrand, K. An Al−Al One-Electron π Bond. *Angew. Chem., Int. Ed. Engl.* **1993**, *32* (3), 388−390.

(18) Sekiguchi, A.; Fukawa, T.; Nakamoto, M.; Lee, V. Ya.; Ichinohe, M. Isolable Silyl and Germyl Radicals Lacking Conjugation with π-Bonds: Synthesis, Characterization, and Reactivity. *J. Am. Chem. Soc.* **2002**, *124* (33), 9865−9869.

(19) Nakamoto, M.; Yamasaki, T.; Sekiguchi, A. Stable Mononuclear Radical Anions of Heavier Group 13 Elements: [$(tBu_2MeSi)_3E^{\bullet}$]·[K+(2.2.2-Cryptand)] (E = Al, Ga). *J. Am. Chem. Soc.* **2005**, *127* (19), 6954−6955.

(20) Li, B.; Geoghegan, B. L.; Weinert, H. M.; Wölper, C.; Cutsail, G. E.; Schulz, S. Synthesis and Redox Activity of Carbene-Coordinated Group 13 Metal Radicals. *Chem. Commun.* **2022**, *58* (27), 4372−4375.

(21) Li, B.; Kundu, S.; Stückl, A. C.; Zhu, H.; Keil, H.; Herbst-Irmer, R.; Stalke, D.; Schwederski, B.; Kaim, W.; Andrada, D. M.; Frenking, G.; Roesky, H. W. A Stable Neutral Radical in the Coordination Sphere of Aluminum. *Angew. Chem., Int. Ed.* **2017**, *56* (1), 397−400.

(22) Kundu, S.; Sinhababu, S.; Dutta, S.; Mondal, T.; Koley, D.; Dittrich, B.; Schwederski, B.; Kaim, W.; Stückl, A. C.; Roesky, H. W. Synthesis and Characterization of Lewis Base Stabilized Mono- and Di-Organo Aluminum Radicals. *Chem. Commun.* **2017**, *53* (76), 10516−10519.

(23) Siddiqui, M. M.; Banerjee, S.; Bose, S.; Sarkar, S. K.; Gupta, S. K.; Kretsch, J.; Graw, N.; Herbst-Irmer, R.; Stalke, D.; Dutta, S.; Koley, D.; Roesky, H. W. Cyclic (Alkyl)(Amino)Carbene-Stabilized Aluminum and Gallium Radicals Based on Amidinate Scaffolds. *Inorg. Chem.* **2020**, *59* (16), 11253−11258.

(24) Koptseva, T. S.; Moskalev, M. V.; Skatova, A. A.; Rumyantcev, R. V.; Fedushkin, I. L. Reduction of CO_2 with Aluminum Hydrides Supported with Ar-BIAN Radical-Anions (Ar-BIAN = 1,2-Bis(Arylimino)Acenaphthene). *Inorg. Chem.* **2022**, *61* (1), 206−213.

(25) Fedushkin, I. L.; Moskalev, M. V.; Lukoyanov, A. N.; Tishkina, A. N.; Baranov, E. V.; Abakumov, G. A. Dialane with a Redox-Active Bis-Amido Ligand: Unique Reactivity towards Alkynes. *Chem. − Eur. J.* **2012**, *18* (36), 11264−11276.

(26) Koptseva, T. S.; Moskalev, M. V.; Baranov, E. V.; Fedushkin, I. L. Reduction of Nitrous Oxide and Binding of Carbon Dioxide by Acenaphthene-1,2-Diimine Aluminum Compounds. *Organometallics* **2023**, *42* (10), 965−970.

(27) Dhara, D.; Endres, L.; Krummenacher, I.; Arrowsmith, M.; Dewhurst, R. D.; Engels, B.; Bertermann, R.; Finze, M.; Demeshko, S.; Meyer, F.; Fantuzzi, F.; Braunschweig, H. Synthesis and Reactivity of a Dialane-Bridged Diradical. *Angew. Chem., Int. Ed.* **2024**, *63* (18), No. e202401052.

(28) Dhara, D.; Fantuzzi, F.; Härterich, M.; Dewhurst, R. D.; Krummenacher, I.; Arrowsmith, M.; Pranckevicius, C.; Braunschweig, H. Stepwise Reduction of a Base-Stabilised Ferrocenyl Aluminium-

(III) Dihalide for the Synthesis of Structurally-Diverse Dialane Species. *Chem. Sci.* **2022**, *13* (33), 9693−9700.
(29) Mandal, D.; Demirer, T. I.; Sergeieva, T.; Morgenstern, B.; Wiedemann, H. T. A.; Kay, C. W. M.; Andrada, D. M. Evidence of Al^{II} Radical Addition to Benzene. *Angew. Chem., Int. Ed.* **2023**, *62* (13), No. e202217184.
(30) Sinhababu, S.; Radzhabov, M. R.; Telser, J.; Mankad, N. P. Cooperative Activation of CO_2 and Epoxide by a Heterobinuclear Al−Fe Complex via Radical Pair Mechanisms. *J. Am. Chem. Soc.* **2022**, *144* (7), 3210−3221.
(31) Sinhababu, S.; Mankad, N. P. Diverse Thermal and Photochemical Reactivity of an Al−Fe Bonded Heterobimetallic Complex. *Organometallics* **2022**, *41* (15), 1917−1921.
(32) Sinhababu, S.; Singh, R. P.; Radzhabov, M. R.; Kumawat, J.; Ess, D. H.; Mankad, N. P. Coordination-Induced O-H/N-H Bond Weakening by a Redox Non-Innocent, Aluminum-Containing Radical. *Nat. Commun.* **2024**, *15* (1), 1315.
(33) Agarwal, R. G.; Coste, S. C.; Groff, B. D.; Heuer, A. M.; Noh, H.; Parada, G. A.; Wise, C. F.; Nichols, E. M.; Warren, J. J.; Mayer, J. M. Free Energies of Proton-Coupled Electron Transfer Reagents and Their Applications. *Chem. Rev.* **2022**, *122* (1), 1−49.
(34) Ramírez-Solís, A.; Boekell, N. G.; León-Pimentel, C. I.; Saint-Martin, H.; Bartulovich, C. O.; Flowers, R. A. I. Ammonia Solvation vs Aqueous Solvation of Samarium Diiodide. A Theoretical and Experimental Approach to Understanding Bond Activation Upon Coordination to Sm(II). *J. Org. Chem.* **2022**, *87* (3), 1689−1697.
(35) Kolmar, S. S.; Mayer, J. M. $SmI_2(H_2O)_n$ Reduction of Electron Rich Enamines by Proton-Coupled Electron Transfer. *J. Am. Chem. Soc.* **2017**, *139* (31), 10687−10692.
(36) Singh, R. P.; Mankad, N. P. Frustrated Al/M Heterobimetallic Complexes (M = Cr, Mo, W) That Exhibit Both Lewis and Radical Pair Behavior. *Inorg. Chem.* **2024**, *63* (40), 18933−18944.
(37) Hubbell, A. K.; Coates, G. W. Nucleophilic Transformations of Lewis Acid-Activated Disubstituted Epoxides with Catalyst-Controlled Regioselectivity. *J. Org. Chem.* **2020**, *85* (21), 13391−13414.
(38) Subasinghe, S. M. S.; Radzhabov, M. R.; Mankad, N. P. Predictive Models for Ligand Effects on a Reactive Al-Containing Radical Intermediate from Multivariate Linear Regression Analysis. *Organometallics* **2024**, *43* (22), 2854−2861.
(39) Subasinghe, S. M. S.; Mankad, N. P. Predictive Models for Metal−Metal Bond Dissociation Free Energies between Aluminum(III) and a Series of Transition Metal Carbonyls. *Polyhedron* **2023**, *245*, No. 116637.
(40) Griffin, L. P.; Ellwanger, M. A.; Clark, J.; Myers, W. K.; Roper, A. F.; Heilmann, A.; Aldridge, S. Bis(Aluminyl)Magnesium: A Source of Nucleophilic or Radical Aluminium-Centred Reactivity. *Angew. Chem., Int. Ed.* **2024**, *63* (22), No. e202405053.
(41) Singh, R. P.; Quirion, K. P.; Telser, J.; Ess, D. H.; Mankad, N. P. Cooperative Heterobimetallic CO_2 Activation Involving a Mononuclear Aluminum(II) Intermediate. *J. Am. Chem. Soc.* **2025**, *147* (15), 12715−12721.
(42) Hannah, T. J.; Chitnis, S. S. Ligand-Enforced Geometric Constraints and Associated Reactivity in p-Block Compounds. *Chem. Soc. Rev.* **2024**, *53* (2), 764−792.
(43) Zou, W.; Mears, K. L.; Fettinger, J. C.; Power, P. P. Sn(II)−Carbon Bond Reactivity: Radical Generation and Consumption via Reactions of a Stannylene with Alkynes. *Chem. Commun.* **2023**, *59* (88), 13203−13206.
(44) Birnthaler, D.; Narobe, R.; Lopez-Berguno, E.; Haag, C.; König, B. Synthetic Application of Bismuth LMCT Photocatalysis in Radical Coupling Reactions. *ACS Catal.* **2023**, *13* (2), 1125−1132.
(45) Mato, M.; Cornella, J. Bismuth in Radical Chemistry and Catalysis. *Angew. Chem., Int. Ed.* **2024**, *63* (8), No. e202315046.
(46) Martínez, S.; Lichtenberg, C. Bismuth-Centered Radical Species: Access and Applications in Organic Synthesis. *Synlett* **2024**, *35*, 1530−1539.
(47) Hasenzahl, S.; Kaim, W.; Stahl, T. Charge and Electron Transfer from Metal-to-Carbon Bonds of Main Group Organometallics MR_n (M = Al, Ga, Zn) to Aromatic N-Heterocycles: Colored Precursor Compounds and Radical Complex Formation. *Inorg. Chim. Acta* **1994**, *225* (1), 23−34.
(48) Hirai, Y.; Murayama, H.; Aida, T.; Inoue, S. Activation of a Metal Axial Ligand Bond in Aluminum Porphyrin by Visible Light. *J. Am. Chem. Soc.* **1988**, *110* (22), 7387−7390.
(49) Wenzel, J. O.; Werner, J.; Allgaier, A.; van Slageren, J.; Fernández, I.; Unterreiner, A.-N.; Breher, F. Visible-Light Activation of Diorganyl Bis(Pyridylimino) Isoindolide Aluminum(III) Complexes and Their Organometallic Radical Reactivity. *Angew. Chem., Int. Ed.* **2024**, *63* (19), No. e202402885.
(50) Onneken, C.; Morack, T.; Soika, J.; Sokolova, O.; Niemeyer, N.; Mück-Lichtenfeld, C.; Daniliuc, C. G.; Neugebauer, J.; Gilmour, R. Light-Enabled Deracemization of Cyclopropanes by Al-Salen Photocatalysis. *Nature* **2023**, *621* (7980), 753−759.
(51) Hao, W.; Harenberg, J. H.; Wu, X.; MacMillan, S. N.; Lin, S. Diastereo- and Enantioselective Formal [3 + 2] Cycloaddition of Cyclopropyl Ketones and Alkenes via Ti-Catalyzed Radical Redox Relay. *J. Am. Chem. Soc.* **2018**, *140* (10), 3514−3517.
(52) Kim, S.; Chen, P.-P.; Houk, K. N.; Knowles, R. R. Reversible Homolysis of a Carbon−Carbon σ-Bond Enabled by Complexation-Induced Bond-Weakening. *J. Am. Chem. Soc.* **2022**, *144* (34), 15488−15496.
(53) Gilbert, M. M.; Trenerry, M. J.; Longley, V. R.; Castro, A. J.; Berry, J. F.; Weix, D. J. Ligand−Metal Cooperation Enables Net Ring-Opening C−C Activation/Difunctionalization of Cyclopropyl Ketones. *ACS Catal.* **2023**, *13* (17), 11277−11290.
(54) Lee, K.; Blake, A. V.; Tanushi, A.; McCarthy, S. M.; Kim, D.; Loria, S. M.; Donahue, C. M.; Spielvogel, K. D.; Keith, J. M.; Daly, S. R.; Radosevich, A. T. Validating the Biphilic Hypothesis of Nontrigonal Phosphorus(III) Compounds. *Angew. Chem., Int. Ed.* **2019**, *58* (21), 6993−6998.
(55) Jazzar, R.; Soleilhavoup, M.; Bertrand, G. Cyclic (Alkyl)- And (Aryl)-(Amino)Carbene Coinage Metal Complexes and Their Applications. *Chem. Rev.* **2020**, *120* (9), 4141−4168.
(56) Abbenseth, J.; Goicoechea, J. M. Recent Developments in the Chemistry of Non-Trigonal Pnictogen Pincer Compounds: From Bonding to Catalysis. *Chem. Sci.* **2020**, *11* (36), 9728−9740.
(57) Lipshultz, J. M.; Li, G.; Radosevich, A. T. Main Group Redox Catalysis of Organopnictogens: Vertical Periodic Trends and Emerging Opportunities in Group 15. *J. Am. Chem. Soc.* **2021**, *143* (4), 1699−1721.
(58) Moon, H. W.; Cornella, J. Bismuth Redox Catalysis: An Emerging Main-Group Platform for Organic Synthesis. *ACS Catal.* **2022**, *12* (2), 1382−1393.
(59) Walsh, A. D. 469. The Electronic Orbitals, Shapes, and Spectra of Polyatomic Molecules. Part IV. Tetratomic Hydride Molecules, AH_3. *J. Chem. Soc.* **1953**, 2296−2301.
(60) Rayner-Canham, G. Isodiagonality in the Periodic Table. *Found. Chem.* **2011**, *13* (2), 121−129.
(61) Boekell, N. G.; Flowers, R. A. I. Coordination-Induced Bond Weakening. *Chem. Rev.* **2022**, *122* (16), 13447−13477.
(62) Bezdek, M. J.; Guo, S.; Chirik, P. J. Coordination-Induced Weakening of Ammonia, Water, and Hydrazine X−H Bonds in a Molybdenum Complex. *Science* **2016**, *354* (6313), 730−733.
(63) Cuerva, J. M.; Campaña, A. G.; Justicia, J.; Rosales, A.; Oller-López, J. L.; Robles, R.; Cárdenas, D. J.; Buñuel, E.; Oltra, J. E. Water: The Ideal Hydrogen-Atom Source in Free-Radical Chemistry Mediated by TiIII and Other Single-Electron-Transfer Metals? *Angew. Chem., Int. Ed.* **2006**, *45* (33), 5522−5526.
(64) Asandei, A. D.; Chen, Y.; Saha, G.; Moran, I. W. Cp_2TiCl-Catalyzed Radical Chemistry: Living Styrene Polymerizations from Epoxides, Aldehydes, Halides, and Peroxides. *Tetrahedron* **2008**, *64* (52), 11831−11838.
(65) McCallum, T.; Wu, X.; Lin, S. Recent Advances in Titanium Radical Redox Catalysis. *J. Org. Chem.* **2019**, *84* (22), 14369−14380.
(66) Lalrempuia, R.; Kefalidis, C. E.; Bonyhady, S. J.; Schwarze, B.; Maron, L.; Stasch, A.; Jones, C. Activation of CO by Hydrogenated Magnesium(I) Dimers: Sterically Controlled Formation of Ethene-

https://doi.org/10.1021/jacsau.5c00352
JACS Au 2025, 5, 2076−2088

diolate and Cyclopropanetriolate Complexes. *J. Am. Chem. Soc.* **2015**, *137* (28), 8944−8947.
(67) Wedal, J. C.; Evans, W. J. A Rare-Earth Metal Retrospective to Stimulate All Fields. *J. Am. Chem. Soc.* **2021**, *143* (44), 18354−18367.
(68) Schäfer, S.; Kaufmann, S.; Rösch, E. S.; Roesky, P. W. Divalent Metallocenes of the Lanthanides − a Guideline to Properties and Reactivity. *Chem. Soc. Rev.* **2023**, *52* (12), 4006−4045.
(69) Bartulovich, C. O.; Flowers, R. A. Coordination-Induced O−H Bond Weakening in Sm(II)-Water Complexes. *Dalton Trans.* **2019**, *48* (43), 16142−16147.
(70) Evans, W. J.; Kociok-Koehn, G.; Leong, V. S.; Ziller, J. W. Reactivity of Hydrazines with Organometallic Samarium Complexes and the X-Ray Crystal Structures of $(C_5Me_5)_2Sm(\eta^2$-PhNHNPh)-(THF), $(C_5Me_5)_2Sm(NHPh)(THF)$, and $[(C_5Me_5)_2Sm]_2(\mu$-η^2:η^2-HNNH). *Inorg. Chem.* **1992**, *31* (17), 3592−3600.
(71) Evans, W. J.; Hanusa, T. P.; Levan, K. R. Synthesis and Structure of an Organosamarium Aryloxide Complex, $(C_5Me_5)_2Sm$-$(OC_6HMe_4$-2,3,5,6). *Inorg. Chim. Acta* **1985**, *110* (3), 191−195.
(72) Evans, W. J.; Rabe, G. W.; Ziller, J. W. Synthesis and X-Ray Crystal Structure of Nitrogen Base Adducts of Decamethylsamarocene: $(C_5Me_5)_2Sm(NH_2CMe_3)$ and $(C_5Me_5)_2Sm(N$-MeIm$)_2$. *J. Organomet. Chem.* **1994**, *483* (1), 39−45.
(73) Evans, W. J.; Seibel, C. A.; Ziller, J. W. Organosamarium-Mediated Transformations of CO_2 and COS: Monoinsertion and Disproportionation Reactions and the Reductive Coupling of CO_2 to $[O_2CCO_2]^{2-}$. *Inorg. Chem.* **1998**, *37* (4), 770−776.
(74) Jaroschik, F.; Nief, F.; Le Goff, X.-F.; Ricard, L. Synthesis and Reactivity of Organometallic Complexes of Divalent Thulium with Cyclopentadienyl and Phospholyl Ligands. *Organometallics* **2007**, *26* (14), 3552−3558.
(75) Yadav, R.; Simler, T.; Gamer, M. T.; Köppe, R.; Roesky, P. W. Rhenium Is Different: CO Tetramerization Induced by a Divalent Lanthanide Complex in Rhenium Carbonyls. *Chem. Commun.* **2019**, *55* (41), 5765−5768.
(76) Yadav, R.; Hossain, M. E.; Paramban, R. P.; Simler, T.; Schoo, C.; Wang, J.; Deacon, G. B.; Junk, P. C.; Roesky, P. W. 3d−4f Heterometallic Complexes by the Reduction of Transition Metal Carbonyls with Bulky Ln^{II} Amidinates. *Dalton Trans.* **2020**, *49* (23), 7701−7707.
(77) Frisch, M. J.; Trucks, G. W.; Schlegel, H. B.; Scuseria, G. E.; Robb, M. A.; Cheeseman, J. R.; Scalmani, G.; Barone, V.; Petersson, G. A.; Nakatsuji, H.; Li, X.; Caricato, M.; Marenich, A. V.; Bloino, J.; Janesko, B. G.; Gomperts, R.; Mennucci, B.; Hratchian, H. P.; Ortiz, J. V.; Izmaylov, A. F.; Sonnenberg, J. L.; Williams-Young, D.; Ding, F.; Lipparini, F.; Egidi, F.; Goings, J.; Peng, B.; Petrone, A.; Henderson, T.; Ranasinghe, D.; Zakrzewski, V. G.; Gao, J.; Rega, N.; Zheng, G.; Liang, W.; Hada, M.; Ehara, M.; Toyota, K.; Fukuda, R.; Hasegawa, J.; Ishida, M.; Nakajima, T.; Honda, Y.; Kitao, O.; Nakai, H.; Vreven, T.; Throssell, K.; Montgomery, J. A., Jr.; Peralta, J. E.; Ogliaro, F.; Bearpark, M. J.; Heyd, J. J.; Brothers, E. N.; Kudin, K. N.; Staroverov, V. N.; Keith, T. A.; Kobayashi, R.; Normand, J.; Raghavachari, K.; Rendell, A. P.; Burant, J. C.; Iyengar, S. S.; Tomasi, J.; Cossi, M.; Millam, J. M.; Klene, M.; Adamo, C.; Cammi, R.; Ochterski, J. W.; Martin, R. L.; Morokuma, K.; Farkas, O.; Foresman, J. B.; Fox, D. J. *Gaussian16 Revision C.01*, 2016.
(78) Grimme, S.; Hansen, A.; Brandenburg, J. G.; Bannwarth, C. Dispersion-Corrected Mean-Field Electronic Structure Methods. *Chem. Rev.* **2016**, *116* (9), 5105−5154.
(79) Grimme, S.; Ehrlich, S.; Goerigk, L. Effect of the Damping Function in Dispersion Corrected Density Functional Theory. *J. Comput. Chem.* **2011**, *32* (7), 1456−1465.
(80) Tomasi, J.; Mennucci, B.; Cammi, R. Quantum Mechanical Continuum Solvation Models. *Chem. Rev.* **2005**, *105* (8), 2999−3094.

https://doi.org/10.1021/jacsau.5c00352
JACS Au 2025, 5, 2076−2088